THE CONTINUOUS HARD X-RAY IMAGER FOR ASTROPHYSICS

Richard E. Rothschild, James L. Matteson, William A. Heindl, and Laurence E. Peterson

Center for Astrophysics and Space Sciences, University of California, San Diego
9500 Gilman Dr., La Jolla, CA 92093-0111

Paul L. Hink
Department of Physics, Washington University
One Brookings Hall, St. Louis, MO 63130

ABSTRACT

CHIP — the Continuous Hard x-ray Imager for astroPhysics) — is a powerful hard X-ray imaging spectroscopy mission, an order of magnitude more sensitive to hard X-rays than XTE, comprised of the Large Uniform Coverage Imager (LUCY) for all-sky coverage and the Deep Extragalactic Survey Imager (DESI) for more sensitive pointed observations. Both instrument complements will utilize the room temperature semiconductor CdZnTe in mosiaced arrays of position sensitive devices in conjunction with coded masks. Each unit will provide imaging from 2–100 keV with ~1 keV energy resolution throughout the entire energy range and few arcminute intrinsic spatial resolution. LUCY will provide 1) a complete flux-limited sample of the hard X-ray contents of our galaxy as well as of the extragalactic sky, 2) alarms and precise positions for transient phenomena on all timescales from seconds to days, and 3) continuous spectral/temporal studies of these objects over a vast range of timescales from seconds to days, to months, to years. DESI will extend LUCY's coverage even deeper by viewing a small portion of the hard x-ray sky (0.01 sr) for background limited studies of individual objects considerably deeper than present or future hard x-ray instruments.

Keywords: x-ray astronomy, x-ray astronomy instrumentation, x-ray spectrometers, spaceborne experiments and missions, semiconductor detectors, detector systems, coded masks, CdZnTe

2. CONCEPT SUMMARY

The **C**ontinuous **H**ard X-ray **I**mager for astro**P**hysics or **CHIP** mission concept for 2-100 keV hard X-ray astronomy combines a powerful hard X-ray imaging telescope (10 times more sensitive than HEXTE or OSSE) and a powerful, continuous, hard X-ray all-sky imager (10 times more sensitive than the ASM on XTE and 3 times more sensitive than BATSE). This mission, , will provide images with 10 arcminute angular resolution of selected portions of the sky 10 times deeper than XTE, will provide high time resolution observations of bright Galactic objects with 10 times better energy resolution at 60 keV than any scintillator mission, and will generate a continuous, hard X-ray flux-limited all-sky survey a factor of 100 deeper than the HEAO-1 13-180 keV survey[1] and 10 times deeper than the HEAO-1 0.25-25 keV survey[2] and 2-10 keV extragalactic survey[3]. This mission will yield spectra and identifications of several thousand extragalactic objects and about one thousand galactic sources, and will provide greater insights into many classes of astronomical object. In addition, the continuous, all-sky imager will observe several hundred gamma ray bursts per year (twice the BATSE rate) and locate them to <100 arcmin^2 (1000 times smaller than the best BATSE derived error boxes). This will undoubtedly advance our knowledge of, if not answer, the question of the origin of gamma ray bursts.

Equally important, CHIP will produce 2-100 keV images and catalogs of the entire sky for comparison with observations made at other wavelengths, just as the Palomar Sky Survey, ROSAT Sky Survey, IRAS Sky Survey, the VLA survey, and EUVE Sky Survey are used today. The >10 keV hard X-ray band is of crucial astrophysical importance, since obscuration by intervening Galactic gas and dust does not limit the view of the galaxy or beyond, and because hard X-ray emission frequently originates close to the primary energy release. Extending observations of cosmic X-ray sources from the conventional 2-10 keV range, where techniques using focusing X-ray optics are readily applied, into the higher energy ranges is a central objective of high energy astrophysics. It is in the tens of keV regime where the production by non-thermal processes becomes dominant over thermal emission in many sources, such as binary X-ray sources, supernovae remnants, active galactic nuclei and clusters of galaxies.. Indeed, this whole regime has been studied only with limited sensitivity and angular resolution thus far, and many studies for future space missions have indicated the important new knowledge of astrophysical phenomena likely to be obtained with modern instruments operating in this range.

3. SCIENTIFIC OBJECTIVES

This decade has seen a revolution in our view of the X-ray sky. This improved vision has derived from a combination of several observational capabilities—more sensitive observations of individual objects, continuous monitoring of large portions of the sky in hard X-rays, a survey of the entire sky in soft X-rays, and the cross correlation of multi-wavelength observations. ROSAT (0.1-2 keV), GINGA (2-40 keV), and now ASCA (0.5-10 keV) provide sensitive, spectroscopic observations of individual objects, giving insight into the mechanisms at work in these high energy sources. The effectiveness of ROSAT and ASCA have been and will continue to be enhanced by the monitoring of the hard X-ray sky by BATSE on CGRO and the WATCH instrument on GRANAT. These instruments have shown the hard X-ray sky to be highly variable and the BATSE instrument presently monitors the hard X-ray sky above 20 keV for bright transients and tracks the variability of the brightest two dozen sources[4]. The power of the synergy between all-sky viewing and pointed missions is clear, and the importance of continuous tracking of known sources, and of promptly alerting the community to a transient in order to allow coordinated observings of such events, has been demonstrated several times over.

The recent ROSAT All-Sky Survey[5] has propelled X-ray astronomy into the realm of optical astronomy by providing large source samples, which may be studied as classes, rather than as individual curiosities. Similarly, missions in the infrared (IRAS) and extreme ultraviolet (ROSAT and EUVE) have been combined with optical surveys (e.g., the Palomar Sky Survey) to allow for multi-wavelength investigations of several classes of objects, with their attendant advances in our understanding of the heavens (e.g., the unified model for Seyferts and AGN[6]). At higher energies, the last complete, full sky surveys were made by the HEAO-1 mission over 15 years ago with the 0.25-25 keV A-1 catalog[2] (842 sources), the 13-180 keV A-4 catalog[1] (72 sources) and the 2-10 keV A-2 extragalactic catalog[3] (85 sources). The XTE All-Sky Monitor will be the next advance with a 2-10 keV catalog and images of the sky that are complete at the few milliCrab level). The XTE ASM, however, will only detect a few hundred sources in the 2-10 keV range, and class studies will be limited by the low number of objects and the narrow energy range. Increasing the number of hard X-ray sources into the thousands for performing class-level studies is essential to understanding global aspects of astrophysical objects and the physics involved.

Progress in the field requires additional capabilites as well. While surveys are necessary to discover new sources, the observations that are essential to study their detailed physics are almost always done with narrow-field, large-area and low-background instruments that obtain good sensitivites in short times. The PCA and HEXTE instruments on the upcoming XTE mission are examples. These large detectors are collimated to 1°, allowing them to study variability on time scales down to <1 ms, but they only observe 1/40,000 of the sky at any time and almost all of the X-ray sky will never be seen by them! Furthermore, since their pencil-beam apertures do not provide imaging, they will become source-confused at sensitivities of a few tenths of a mCrab (PCA) and ~1 mCrab (HEXTE), and will not be able to study fainter sources. Imaging is essential for observations with better sensitivity.

Our understanding of the physics of astrophysical sources depends on observations with enough spectral resolution to reveal details of their photon spectra. We now know that narrow cyclotron absorption lines and sharp spectral breaks often occur in the 10 keV to 100 keV range. Narrow emission lines at 68 and 78 keV are expected from ^{44}Ti in galactic supernovae. Reflection spectra in AGN contain Fe lines and edges as well as broad continua. The energy resolution of the typical NaI(Tl) detector, 10 keV at 60 keV, is not adequate for detailed studies of these lines. A resolution of ~1 keV is required. At lower energies many astrophysical settings produce atomic lines, the iron line complex at about 6 keV being the most obvious. These lines are being studied in detail with fine resolution by ASCA and they will be a major objective of the AXAF and Astro-E. Here we are primarily concerned with hard X-ray astronomy and the extension of >20 keV source spectra down to the classical, 2-10 keV X-ray domain. It will be adequate to have knowledge of the strength of the iron line complex, but not to perform detailed spectroscopy. Again, an energy resolution of ~1 keV would be appropriate.

3.1 Complete extragalactic sample

The last complete high latitude survey of the 2-10 keV emission from clusters of galaxies and active galaxies[3] can be used to estimate the number of extragalactic sources as a function of their strength. The small number of detections of extragalactic objects at 50 keV[1] has not supported estimates at hard x-ray energies. Extending the HEAO-1 results below 1 mCrab on the assumption that luminosity functions do not affect the results predicts the CHIP All-Sky Survey will yield ~4x10^3 extragalactic sources and the deeper survey with the pointed instrument will yield another 4-5x10^3 extragalactic sources. This large sample can then be divided into subsamples based upon various source characteristics, such as redshift, radio loudness, class of object, etc., which will contain significant numbers. When cross correlated with data at other wavelengths, detailed studies of these samples will provide powerful diagnostics of emission mechanisms, mass distribution, evolution, and beam formation processes. Luminosity functions in the X-ray range, which were limited in the past by low sample counts, will be constructed in order to study the evolution of clusters of galaxies, Seyfert galaxies, etc. Quasars will be detected to a redshift of 2 or more, and the predicted spectral break in the 50-200 keV range will redshifted directly into the CHIP energy range.

3.1.1 Classes of active galactic nuclei

The X-ray spectra of active galactic nuclei (AGN) in the 2-100 keV energy band are relevant not only as a probe of the AGN central engine but also for their contribution to the diffuse X-ray background at the energies above 20 keV where extrapolation of lower energy results become less certain. The OSSE observations of IC 4329A and NGC 4151 show that the high energy spectrum rolls over far below an MeV, whereas the few sources with Ginga and OSSE observations show a great deal of diagnostic structure in the 2-100 keV energy band: an iron line (6.4-6.7 keV) which may result from fluoresence in both the accretion disk and the thick torus surrounding the central engine; a component above 10 keV produced by reflection of the primary X-ray source off the accretion disk; and the primary X-ray source which might combine both nonthermal emission and thermal Comptonization. The combined Ginga-OSSE spectra show significant spectral differences between the small number of radio quiet Seyfert 1s (reflection component and a soft $\alpha = 0.9$ primary spectrum), radio loud Seyfert 1s (little or no reflection and a harder $\alpha = 0.7$ primary spectrum) and Seyfert 2s (large neutral absorption and possibly a primary spectrum harder than $\alpha = 0.9$) which result from orientation effects in unified models (e.g., between radio quiet Seyfert 1s and Seyfert 2s) or different AGN classes (e.g., between radio quiet and radio loud Seyfert 1s). Accumulating a larger source sample in this crucial energy band will better constrain models of the inner region of AGN, and space instruments with substantial improvements in energy resolution, sensitivity above 10 keV, and imaging at better angular resolution than will be possible with XTE are essential to further progress in understanding AGN.

3.1.2 Diffuse x-ray background

The origin of the diffuse X-ray background is one of the long standing questions in astrophysics. Sensitive imaging instruments, e.g., ROSAT and Einstein, have identified the source of most of the background below 3 keV. However, at higher energies its source is less certain. Indeed, the spectra of the best studied sources—Seyfert 1s and QSOs—are not hard enough above 3 keV to produce the background. Consequently, other extragalactic sources have been proposed. In particular, the unified AGN model suggests that Seyfert 2s could be the dominant source: the torus which obscures the optical, UV and low energy X-rays may be transparent to high energy X-rays. The sum of sources with different low energy cutoffs could result in the observed hard background between 3 and 40 keV. This conjecture has been tested with four Seyfert 2s (including NGC 4151, which is a Seyfert 1.5), and a much larger sample is clearly necessary. CHIP would provide the large samples of extragalactic object spectra necessary to test various models by detecting several thousand sources and determining spectral parameters for several hundred with good statistical significance. These observations would be a tremendous advance in our understanding of AGNs and the hard X-ray diffuse background.

3.1.3 Clusters of galaxies

Clusters of galaxies are extended (core radii ~250 kpc) and luminous ($L_{2-10keV}=10^{43.5-45}\,\mathrm{erg\,s^{-1}}$) X-ray sources exhibiting thermal emission from gas at temperatures ~3–10 keV. The bulk of this emission is at the low end of the CHIP energy range, but a few clusters have been detected above 10 keV. At least two components which appear as power laws are expected to contribute at higher energies: 1) emission components above 10 keV due to the presence of AGNs (eg. NGC 4388 in Virgo, NGC 1275 in Perseus), and 2) inverse Compton scattering of the cosmic microwave background radiation by cluster electrons responsible for the radio emission. When combined with radio data, hard X-ray detections or upper limits above 20 keV can be used to constrain the astrophysically important intracluster magnetic field strength and electron energy density. Since nearby Abell clusters (z~0.01) subtend angular diameters of ~30 arcmin, DESI will be able to resolve the AGN in these clusters and correct for their contribution to the overall cluster flux in order to reveal the inverse Compton component. Even without these high energy components, the improvement represented by the CHIP sensitivity over previous 2–10 keV studies of clusters will allow a number of evolutionary questions to be addressed, such as why high luminosity clusters ($L_x > 8 \times 10^{44}\,\mathrm{erg\,s^{-1}}$) appear to be less common at redshifts $z >0.06$. With a core radius of 2 arcmin, clusters at z~0.1 will appear essentially as a point source to instruments with few arcmin spatial resolution. Extending the results on these objects to 10 keV indicates that CHIP will provide a sample of hundreds.

3.2 Complete galactic inventory

Previous Galactic surveys have mapped the galactic plane to a flux limit of roughly one mCrab on the 2-10 keV band, and 10 mCrab 15-80 keV. At this flux limit a source of luminosity $5\text{x}10^{36}$ ergs/s is just visible at 20 kpc., thus existing surveys can be considered complete for sources of this luminosity and above, but partial for less luminous sources. At 0.1 mCrab the luminosity limit is $5\text{x}10^{35}$ ergs/s, and more, fainter sources can be detected. Using the sample of 26 accretion-driven X-ray pulsars[7] for which 18 have distances and luminosities, we estimate that the class of accreting pulsars observed above 0.1 mCrab can be increased from 26 to a number between several hundred and several thousand. By dividing these sources into massive and low mass systems, into wind and disk accreters, and into sub classes based upon quasiperiodic oscillation phenomenology, to say nothing of multiwavelength studies, we will obtain unprecedented insights into these laboratories for condensed matter and plasma physics.

3.2.1 Black hole physics

Hard X-ray observations of stellar-sized black holes can yield unique information on matter and radiation in deep gravitational wells. Many X-ray obserations of Cygnus X-1, the exemplar of X-ray emitting black hole candidates, have show a confusing richness of temporal and spectral behavior. Many attempts have been made to categorize its emission into "states", but the number of identified states so far is embarrasingly close to the number of sensitive observations. Other black hole candidates, although observations are sparser for these, show the likelihood of a similar richness of X-ray behavior. Although many models have been proposed over the years to describe the emission region geometry and radiation, the observed variety presently poses severe challenges.

The recent Mirabel sources also show complex and tantalizing radio emission. The 12.5 kpc. distance to GRS1915+105 requires it to have a hard X-ray luminosity of $\sim 3 \times 10^{38}$ erg/s when it is active, making it one of the most luminous sources in the Galaxy. It represents the prototype of a new class of astrophysical object, one that is ideally suited for studies with CHIP. At the time of the radio outburst GRS1915+105 was known to be in a period of high X-ray luminosity, and it is known to have periods of high flux, of about 50 mCrab. With CHIP's sensitivity it will be possible to make a detailed study of its X-ray intensity and spectra, and correlate these with radio outbursts and ejection events as measured by the VLA. This should give new insights into the nature of jet acceleration processes and the nature of the central object and its environment, and the results can be expected to aid the study of quasars. It is also reasonable to expect that there are other such objects in the Galaxy and

CHIP's sensitivity would allow an object 25 times weaker to be studied with 1 day time resolution. Indeed, two strong, variable gamma ray sources, 1E1740.7-2942 and GRS1758-258, have been shown to have radio jets, which suggest the ejection of relativistic plasma. CHIP can uniquely and powerfully contribute to the quantity and quality of the temporal and spectral data from which phenomenological study can lead to solid classification and from this to convincing models of structures and radiation processes at deep gravitational potentials.

3.2.2 Accreting pulsar physics

The number of X-ray emitting accreting pulsars currently known in the galaxy is well above thirty[8] and increasing. New observations continue to surprise: long term timing studies have identified orbital decay in several systems; cyclotron lines at energies from 10 to >50 keV are firmly identified now in the spectra of several pulsars; and in Her X-1 a long suspected correlation between pulse shape and the 35 day cycle has been decisively confirmed with Ginga data. In the last case, this association is evidence of a causal connection between the overall precession of the accretion disk and the formation of the pulsation pattern just above the magnetic poles of the neutron star. While XTE will provide important detailed comparisons with physical models, the next observational advance requires measurements of line profiles (typically 10 keV wide) and their variation with pulsation phase in many objects. The CHIP sensitivity to weak sources will permit searches for different signatures of the teraGauss fields, such as emission features in Be binary systems. Such observations require significantly better energy resolution, of the order of a few keV, than can be provided by traditional scintillators and proportional counters. Furthermore, broad band energy coverage will be required to enable the simultaneous detection and tracking of harmonics, which will provide additional constraints on the magnetic field strength, the column temperature, and the electron column density.

3.3 Long term monitoring of the hard x-ray sky

Throughout the history of satellite missions in X-ray astronomy, monitoring large parts of the sky has provided bonanzas in astrophysics due to the highly variable nature of most X-ray sources. Extended observations have discovered many transient events and state variations. Long term monitoring of binary sources has revealed cyclic variability on months or longer time scales[9] attributable to accretion disk precession, Be-neutron star binaries with eccentric orbits, neutron star precession, and other scenarios. Tracking of spin frequencies versus time and versus luminosity has proven to be a powerful tool in understanding both the mass transfer (i.e., wind fed or disk fed) and the accretion torques in neutron star binaries. Variations in X-ray flux, low energy absorption, and pulse fractions from neutron stars in eccentric orbits around Be stars as a function of separation can be used to address questions of acceleration mechanisms and shocks in O and B star stellar winds.

Continuous monitoring of large fractions of the sky has brought us the bright X-ray transients that allow for the investigation of physical processes under differing conditions of luminosity within the same object, the identification of numbers of black hole candidates, and the eccentric Be-star binary systems with periodic and episodic outbursts at periastron passage and other points in the orbit. Weak transients have recently added to our understanding of the Galactic ridge components. The Galactic ridge is a complex X-ray emitting region requiring hard X-ray imaging observations because the n_H value through the galactic plane is larger than 10^{22} cm^{-2} so low energy X-rays are heavily absorbed. New hard X-ray transients found in the plane are very likely to be X-ray pulsars, and, therefore, constant monitoring could reveal a class of low luminosity transient X-ray pulsars dominating the Galactic ridge emission. Fast transients that last for less than a day, and nominally less than a few hours, are estimated to occur 10^{3-5} times per year with fluxes on the order of 10^{-10} ergs s^{-1}. Flare stars and RS CVn systems are generally found to be associated with this phenomenon, but this is based on small samples. These, too, may be constituents of the Galactic ridge, and a large sample is required to understand their flaring and identify the processes involved. Continuous viewing of the entire sky is essential for detecting this short lived phenomenon. CHIP will monitor the hard X-ray sky at a factor of 50 better sensitivity than BATSE, and over the 2-100 keV range this will provide continuous data on hundreds of variable sources.

3.4 Gamma ray bursts

More than twenty years after their discovery, the origin of gamma ray bursts remains one of the most persistent mysteries in astrophysics. BATSE observations[10] have opened the exciting possibility that they may come from cosmological distances. In order to solve this mystery, we need to determine burst positions with much greater precision. These crucial measurements will enable us to: 1) determine whether any burst error boxes are coincident as would be expected if the sources produce repeated bursts as has been suggested from analyses of the BATSE data, and 2) have positional coincidences with particular astronomical objects. This cannot be done with existing burst position determinations. The BATSE positions have systematic uncertainties of $4°$ to $26°$. With such positions we obviously can not identify possible sources, nor can we even determine whether there are repeated bursts from the sources, since in the BATSE sample, the mean separation between random positions on the sky is less than the minimum uncertainty. In the last 16 years the interplanetary networks of burst detectors have determined 33 burst positions with uncertainties less than 150 arcmin^2, but these have not yielded counterparts and the effective temporal and spatial coverage is so low that this sample does not provide a significant test of burst repetition. Similarly the X-ray and UV detectors on the forthcoming HETE mission, which have imaging capabilities of $\sim$ 10 arcmin^2 in the 2 to 10 keV band and $\sim$ 0.1 arcmin^2 in the UV band, have only a $\sim$ 2 sr field of view. Thus, with Earth occultation and various deadtimes, these detectors will be able to observe any particular point in the sky only about 10% of the time, severely reducing their effectiveness in testing burst repetition. If bursts produce optical flashes, HETE may be able to get a few very good positions.

The CHIP continuous all sky imager, with nearly 90% coverage of every point in the sky due to the optimal many-day orbit, will detect roughly 700 bursts per year with positional resolution of $<$ 100 arcmin^2. With twice the number of bursts per year as BATSE, correlations with known distributions, such as galaxies within 20 Megaparsecs, will be powerful tests of theories of origin. This will also place very tight limits on repeating sources. Practically, however, one needs $<$1 arcmin^2 error boxes for a meaningful search for a counterpart. This will be possible for the very brightest of bursts ($>100\sigma$ detections) which CHIP will detect at a rate of $\sim$30/year. For each burst detected, we will investigate the pre- and post-burst data for evidence of additional processes, such as, precursors and afterglow. Since magnetized neutron stars are the only known anchors of $\sim 10^{12}$ Gauss fields, observations of cyclotron absorption features at tens of keV were a major argument that bursts originate on Galactic neutron stars. However, BATSE has not detected any such lines calling the reality of these features into question. CHIP will have the sensitivity and energy resolution to answer this question with the large sample of gamma ray bursts expected. In addition to detecting spectral lines, CHIP will determine the shape of the burst continuum. Since the spectrum reflects the emission processes, a more accurate characterization of the spectrum will better constrain physical models, including ones with multiple components.

3.5 Nucleosynthesis in galaxy

^{44}Ti is predicted to be produced in supernovae in amounts that range from $\sim 10^{-4}$ $M_\odot$ in Type II SN and deflagration models of Type Ia, to 5×10^{-4} $M_\odot$ in detonation models of Type Ia and up to 9×10^{-3} $M_\odot$ in Type Ib. ^{44}Ti decays with a 78 year mean life, always producing three gamma rays at 68, 78, and 1157 keV. With a galactic supernova rate of $\sim$1/50 years, we expect $\sim$ 5 SNRs with a flux above $\sim 10^{-5}$ photons/cm^2-s, and the ^{44}Ti gamma rays offer an excellent method for finding these events. That this is, in fact, possible was recently demonstrated by the discovery of the 1157 keV gamma ray from Cas A (Type II, age $\sim$ 300 yrs, distance $\sim$ 3 kpc) by the COMPTEL on CGRO. Suitably resolved measurements of the widths of the lines can discriminate between detonation models ($\sim$10% width) and deflagration models ($\sim$4% width). The LUCY sensitivity to a 4% broad line at 78 keV will be 1×10^{-6} photons cm^{-2} s^{-1} in one year. This is a factor of 6 better than the planned sensitivity of the INTEGRAL's gamma ray spectrometer Galactic survey (5x10^6 s on any source), and should result in the discovery of many recent supernovae. Candidate supernovae could be confirmed by DESI with a 1-2 week observation.

4. THE CHIP MISSION CONCEPT

CHIP contains an array of wide field of view telescopes that will image the entire sky and a pointed, small field of view telescope for deeper and faster observations. The instruments' sensitivities are given in Table 1 and

Table 1: CHIP Scientific Capabilities

Instrument	Large Uniform Coverage Imager (LUCY)			DEep Survey Imager (DESI)		
Sensitivity[a]	One Hour	One Day	One Year	One Minute	One Hour	Two Weeks
2-10 keV	3 mCrab	700 μCrab	40 μCrab	3 mCrab	400 μCrab	20 μCrab
10-30 keV	6 mCrab	1 mCrab	60 μCrab	7 mCrab	1 mCrab	50 μCrab
30-90 keV	10 mCrab	2 mCrab	100 μCrab	30 mCrab	4 mCrab	200 μCrab
Angular Resolution	30 arcminutes			10 arcminutes		
Field of View	all-sky, continuous			5°x5°		

[a] 1 mCrab = 2×10^{-11} erg cm^{-2} s^{-1} (2-10 keV),
1×10^{-11} erg cm^{-2} s^{-1} (10-30 keV),
1×10^{-11} erg cm^{-2} s^{-1} (30-90 keV)

Figure 2. CHIP would preferably be placed into a many-day orbit that takes it far enough from the Earth so that its view of the sky is relatively unobscured and it is outside the trapped radiation belts. The many-day orbit, similar to that of EXOSAT, will allow for direct satellite to ground telemetry operations. The CHIP would be operated in a three axis stabilized mode with the DESI pointing direction changed about once a week. This provides for ~50 deep DESI surveys per year and for the various portions of the sky to be viewed by different LUCY telescopes to help minimize systematic uncertainties. Ground-based changes in the observing plan can be initiated in less than one day to re-orient the CHIP in response to transient occurrences. However, normal scheduling requires re-orientation on weekly timescales, thus minimizing operational costs. The data will be processed rapidly to provide all-sky monitoring alarms to the world community of astronomers and to other observatories that desire to take advantage of them. In addition, the data from LUCY will be available to those wishing to carry out investigations, such as, comparing X-ray images with those at other wavelengths. Daily, monthly, and yearly maps of the ENTIRE X-ray sky will be available for the astrophysics community, just as the Palomar Sky Survey, the ROSAT pointed observation database, the EUVE Sky Survey, and the IRAS Sky Survey are today. CHIP's sensitivities over the 2-100 keV energy range guarantee overlap and complementarity at lower energies with ROSAT, ASCA, AXAF, and XMM missions, and at the same time provide links to CGRO and INTEGRAL observations at higher energies.

4.1 The large uniform coverage imager (LUCY)

The baseline concept for LUCY is an array of 18 identical, coded mask telescopes with CdZnTe detector planes that have 0.5 mm position resolution. Figure 1 shows an individual LUCY telescope and Table 2 lists the basic parameters of LUCY. Each unit contains a detector array composed of nine 100 cm^2 modules (described below) forming a 900 cm^2 unit. Approximately 26 cm above the detector plane is a square pixel uniformly redundant array (URA) coded mask measuring 60 cm on a side. This mask consists of 2$\times$2 repetions of a single URA unit pattern to provide a $60^\circ \times 60^\circ$ field of view. The mask is composed of 2 mm square cells of 0.6 mm thick tungsten to provide 26 arcmin angular resolution. The large field of view of LUCY makes it important to keep the coded mask thin in order to avoid vignetting of the mask pattern. For this reason, and because the LUCY background is strongly dominated by diffuse flux, the mask is not graded. A passive $60^\circ \times 60^\circ$ collimator above the detector plane sharply reduces the diffuse background from outside of the fully coded field of view with only a modest cost in sensitivity at the field edges. The sides and rear of the detectors are both passively and actively shielded to reduce backgrounds from internal flux and from events caused by charged particles. A single LUCY module has a mass of 24 kg.

The baseline LUCY angular resolution is a trade off between source confusion and detection sensitivity. In order to produce a complete flux-limited survey with limiting sensitivity on the order of 0.1 mCrab or less, a 1 sr ($60^\circ \times 60^\circ$) field of view is required, and would contain a few hundred sources, or about one per ten resolution elements, as is appropriate for a confusion limited situation. The 50 μCrab confusion limit for the 26 arcmin angular resolution of the LUCY will be reached in a little more than a year's operation in the 2-10 keV range.

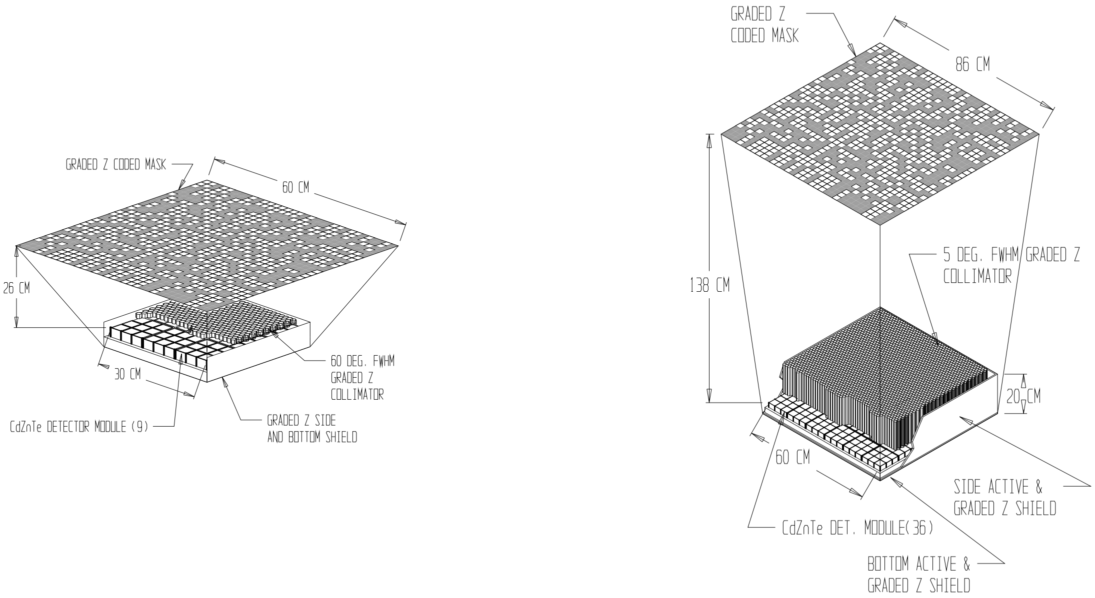

Figure 1: One of eighteen LUCY units and the DESI telescope. In both instruments, the detector plane consists of CdZnTe which is exposed to the sky through a coded mask. In each case, a subcollimator reduces the aperture flux component of the background. For clarity, a coarse mask pattern is shown. The actual mask pixel sizes are 2 mm and 4 mm for the LUCY and DESI respectively Table 2 summarizes the instrument parameters.

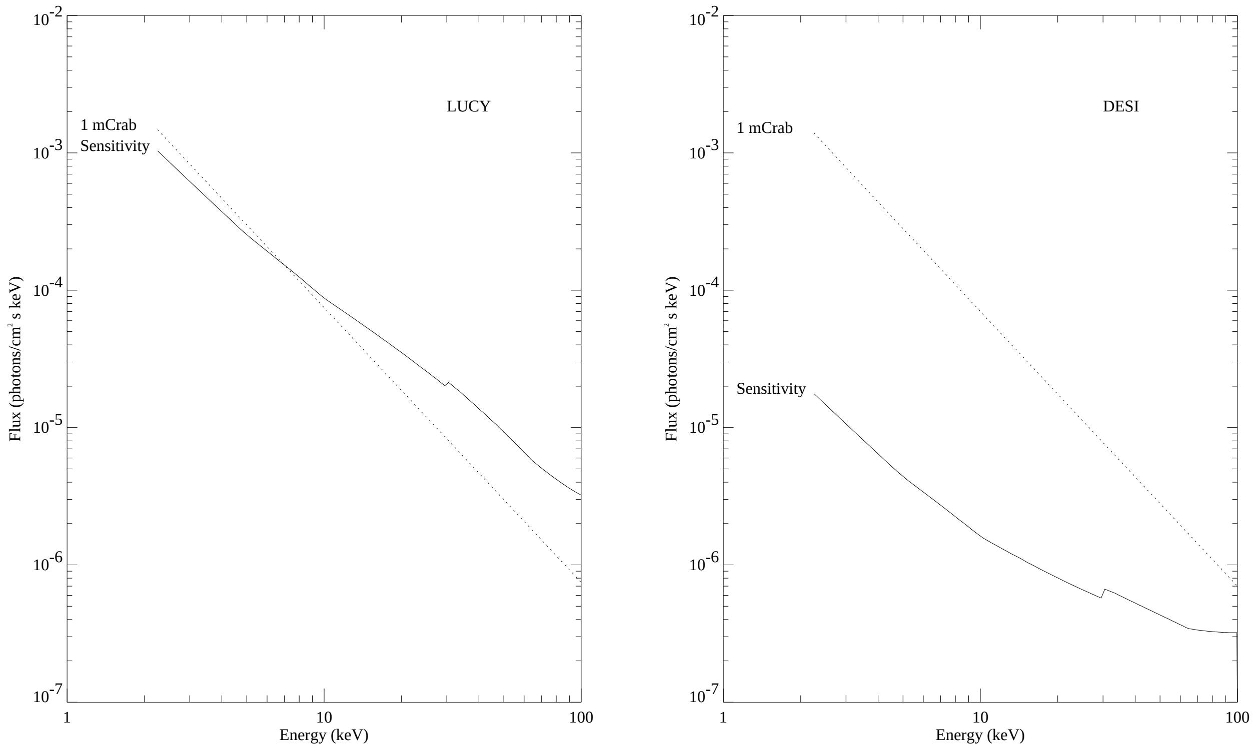

Figure 2: Sensitivity estimates for the LUCY for a 10^5 s and the DESI for a 10^6 s observation respectively. The LUCY will reach a sensitivity of $\sim$1 mCrab in one day and <0.1 mCrab in one year. The DESI will reach a sensitivity of $\sim$30 μCrab and still not be confusion limited in $\sim$2 week.

At that time the 10-30 keV ultimate sensitivity is $\sim$60 μCrab, and at higher energies, a sensitivity of 0.1 mCrab will be realized. In Figure 2, we show the estimated sensitivity of the LUCY for a 10^5 s observation.

4.2 The deep survey imager (DESI)

The DESI consists of 36 100 cm^2 CdZnTe modules totalling 3600 cm^2 and an 86 cm$\times$86 cm coded mask 138 cm above the detector plane with 0.5 mm positional resolution which gives DESI $\sim$10 arcmin angular resolution over a 5° fully coded field of view for 4 mm elements (pixels). Table 2 lists the basic parameters of the pointed DESI telescope. The DESI coded mask is a "graded-Z" sandwich of tungsten, tin, copper, and aluminum. Grading the mask reduces the background component from K fluorescence photons produced after primary X-ray interactions in the mask. In order to balance the goals of wide field imaging with those of high sensitivity deep pointings, a graded-Z collimator with a 5° full width at half maximum (FWHM) response is used to reduce the diffuse background flux incident on the detector. This is especially useful for minimizing flux from within the partially coded field of view which contains a significant level of diffuse emission and may contain point sources which can cause undesireable artifacts in the image reconstruction. The DESI mass is 76 kg.

The DESI angular resolution allows it to perform deeper surveys on selected portions of the sky and detailed spectral investigations of sources weakly detected by the LUCY. In order to go 5 times fainter than LUCY, a confusion limit of 20 μCrab requires an angular resolution of 20 arcmin. Figure 2 shows the sensitivity of the DESI for a 10^6 s observation. The 20 μCrab sensitivity (2-10 keV) is reached in two weeks and this would yield $\sim$60 μCrab sensitivity in the 10-30 keV range, and $\sim$0.20 mCrab in the 30-90 keV range. A 75 msr field of view (5°x5°) at this level will yield 25 AGN or 1 per square degree. Thus, over a 5 year mission, $\sim$200 pointings will

Table 2: LUCY and DESI Instrument Parameters.

		LUCY	DESI
Number of units		12-18	1
Detector plane	CdZnTe	30 cm × 30 cm	60 cm × 60 cm
		1.5 mm thick	1.5 mm thick
	detector contacts	500 μm pitch	500 μm pitch
		x, y readouts	x, y readouts
Mask	dimensions	60 cm × 60 cm	86 cm × 86 cm
		0.6 mm thick	1.6 mm thick
	pixel size	2 mm × 2 mm	4 mm × 4 mm
	material	W	graded Z:
			0.6 mm W, 0.6 mm Sn,
			0.2 mm Cu, 0.2 mm Al
	detector/mask distance	26 cm	138 cm
Collimator	material	W	graded Z
	geometry	hexagonal cylinders	hexagonal cylinders
		1.3 cm flat to flat	1.3 cm flat to flat
		1.1 cm high	14.5 cm high
Imaging	Field of View	60° × 60°	5° × 5°
	Angular Resolution	26 arcmin	10 arcmin
	Point Source Location	~5 arcmin (10σ source)	~1 arcmin (10σ source)
Spectra	Energy Range	2–100 keV	2–100 keV
	Energy Resolution	~1 keV (constant)	~1 keV (constant)

yield ~5000 AGN. This extraordinary performance will provide excellent overlap with the higher performance, narrower field of view, ASCA, AXAF, XMM, Spectrum X/Γ, and Astro-E at 2-10 keV, while extending the spectra as much as an order of magnitude higher in energy.

4.3 Coded Mask Technique

A coded-aperture telescope consists of two primary components: a position sensitive detector plane and a "mask" of opaque and transparent cells. The mask is typically built on a rectangular grid with some cells empty and others filled with X-ray absorbing material, for example lead or tungsten. The detector views the sky through the mask, such that each source in the field of view casts a shadow of the mask on the detector plane. A suitably chosen pattern of open and closed mask cells allows a unique reconstruction of the source distribution (i.e. a sky image) from the measured shadow pattern. Several instruments in the past decade (e.g. the Spacelab-2 X-ray Telescope, the balloon borne instruments GRIP and EXITE, and SIGMA and ART-P on GRANAT) have successfully demonstrated the ability of telescopes based on the coded-aperture principle to produce high resolution images at energies beyond 10 keV where grazing incidence mirrors become impractical. They have also shown that this technique can measure independent spectra and light curves for multiple sources in a single field of view.

4.4 CdZnTe Detector Status

In the past few years there has been significant work done on CdTe and CdZnTe detectors. A number of groups are looking into the use of CdZnTe for gamma ray and X-ray astronomy. CdZnTe implies an alloy composed of 80% CdTe and 20% ZnTe. One of the most attractive features of CdZnTe is its high bandgap, 1.6 eV, which allows room temperature operation. This differs from other solid state detectors such as Ge and Si, which have bandgaps of 0.66 and 1.22 respectively, and require heavy and expensive cryogenics during operation to minimize noise. Other attractive features of CdZnTe are its high average atomic number, 48, and its density, 5.8 g/cm^3. Both of these characteristics are important for detection of high energy X-rays. Since photoelectric absorption

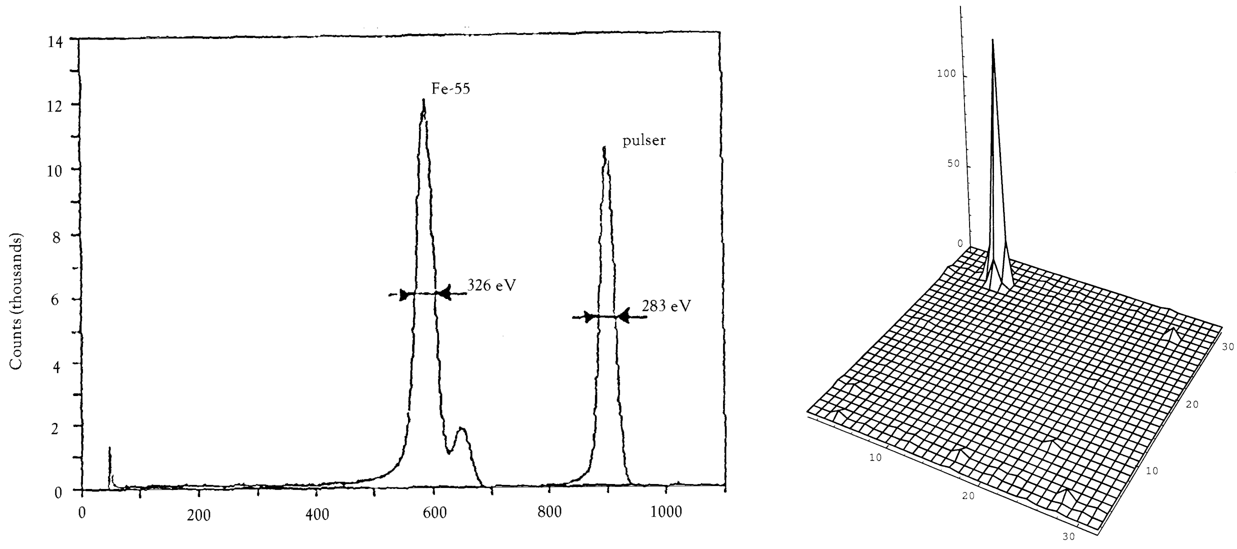

Figure 3: Energy and position response of CdZnTe Detectors. 1) Pulse height spectrum of an ^{55}Fe source in a 2 mm × 2 mm detector. 2) A pinhole camera image of an ^{241}Am source taken with a 35 mm × 35 mm detector.

dominates up to energies of > 250 keV, CdZnTe should be an ideal material for a position sensitive detector over the 2–100 keV energy range. The detection efficiency for a standard 1.5 mm thick detector is 75% at 100 keV, allowing operation at higher energies if desired. CdZnTe detectors are also available with very fine position resolution, demonstrated to $< 400\,\mu$m. The background activation of CdZnTe is similar to the typical alkali halides, such as CsI and NaI, with the exception of the high neutron cross-section of Cd–113 which results in > 500 keV gamma-rays being promptly produced by neutrons of E < 1 eV. This should not be too severe in orbit since the typical flux of neutrons in this energy range is quite low, and can be minimized by judicious choice of orbital parameters.

In Figure 3 we plot the spectrum of an ^{55}Fe source (peaks at 5.9 and 6.5 keV) and test pulser using a commercially available preamplifier[11,12]. The energy resolution, 325 eV FWHM, is limited by preamplifier noise. This resolution is better than gas scintillation counters and is approaching that of Si and Ge solid state detectors. Bias voltages required on these detectors are typically only 400V as compared to 1000 V for gas counters and 2500–4000V for Ge. At higher energies CdZnTe detectors begin to exhibit incomplete charge collection of the holes. However, it has recently been reported that this charge defect phenomenon can be dramatically reduced by either applying a special biasing scheme to the detector, or by using a position sensitive detector with a stripe/pixel width that is narrower than the thickness of the detector. Energy resolution of 1 keV FWHM from 2–30 keV should be obtainable in a space quality detector system. Above 30 keV the energy resolution would degrade due to incomplete charge collection, being roughly 3% FWHM from 30–100 keV.

4.5 Sensitivity estimates

The sensitivity of coded aperture telescopes are limited both by statistical and systematic effects. In the following sections, the most important of these are considered.

4.5.1 Detection sensitivity

For a coded aperture telescope, the minimum source intensity which can be detected at a given statistical significance can be expressed as:

$$F_K(ph/(cm^2\ s\ keV)) = \frac{K}{\epsilon\eta_{pix}\eta_{mask}(1-t_{mask})t_{coll}t_{pass}}\sqrt{\frac{B_{int}+\epsilon\eta_{mask}\frac{G}{A}B_{diff}}{\Delta EA\tau}} \quad (1)$$

whereF_K = flux which can be detected at a statistical significance of K σ, K = statistical significance of the detection, ϵ = photon detection efficiency, η_{pix} = loss of sensitivity for sources not centered on a sky pixel, η_{mask} = fraction of mask cells which are open, t_{mask} = fraction of photons transmitted by closed mask cells, t_{coll} = transmission coefficient of the collimator as a function of off-axis angle, t_{pass} = transmission of absorbing materials (e.g. the mask support plane) in the detector aperture, B_{int} = internal detector background (cts/(cm^2 s keV)). G = acceptance of the mask/collimator/detector combination (cm^2 sr), A = detector geometrical area, B_{diff} = diffuse X-ray background photons cm^{-2} s^{-1} keV^{-1}sr^{-1}, ΔE = energy band of the detection, and τ = livetime of the observation. Of these quantities, ϵ , t_{mask}, t_{coll}, t_{pass}, B_{int}, and B_{diff} are energy dependent.

The loss of sensitivity for sources not at sky pixel centers can be minimized by employing detector pixels which are smaller than the mask pixels. The factor of 4 to 8 oversampling in our instrument concept assumes that this effect is very small. For background limited observations (nearly always the case in hard X-ray astronomy), masks which are half open are statistically optimal, so η_{mask} is ~0.5. In the CHIP energy band, it will be possible to design masks with essentially no transmission, making $(1-t_{mask})$ nearly unity. Based on our experience building collimators for the HEXTE, $\eta_{coll} = 0.9$ for on axis sources. Passive material in the field of view will be kept to a minimum and consist of only low Z elements, so that at all but the lowest energies, t_{pass} will be ~1, and η_{pix} = is about unity. For the diffuse background contribution the analytical fits of HEAO-1 data were used. Scaling from the HEAO-1 A2, HEXE on Mir/Kvant, and HEXTE on XTE experiments, we estimated the internal background component to be approximately constant over the 2 – 100 keV band with a flux of 3 × 10^{-4}(cts/(cm^2 s keV)).

4.5.2 Coded mask sensitivity

It is important to note that equation 1 only includes the contribution of photon statistics to the sensitivity. There are at least two important systematic effects which must also be considered. In order for a source to be imaged efficiently by a coded aperture telescope, its flux must be great enough so that most mask pixels are sampled (i.e. hit) by one or more source photons. If this doesn't occur, then the mask pattern is incompletely sampled for that source, and it is not perfectly imaged. This is primarily a concern for detecting unknown sources. It results in a gradual loss of sensitivity at low source flux and may be a stronger limit on instrument sensitivity than equation 1. The limiting flux, F_p, from this consideration is:

$$F_p(ph/(cm^2\ s\ keV)) = \frac{N_p}{\Delta E\tau A_{pix}} \quad (2)$$

Where N_p is the required mean number of photons per mask pixel and A_{pix} is the geometric area of a pixel. Because F_p is proportional to $1/\tau$, by setting $F_p = F_K$, we can derive a minimum observation time for which F$_p$ does not limit the flux sensitivity.

4.5.3 Signal to noise sensitivity

Another systematic effect associated with the use of coded masks is mainly important in the LUCY. In order for a hard X-ray instrument to achieve its intended long term sensitivity, sources whose signal is much less than 1% of background must be detectable. Systematic spatial variations in the detector background must then be efficiently subtracted. Fortunately, most of these variations are caused by the detector internal background, and the LUCY background is dominated by diffuse flux. However, without the benefit of mask-antimask observations to directly subtract these variations, some form of flat-fielding of the detected shadow pattern must be carried out. This has been done successfully in the NaI coded mask telescopes SIGMA and EXITE. We anticipate that it will also be possible for the CHIP CdZnTe detector modules.

5. REFERENCES

1. Levine, A.M. et al., "The HEAO 1 A-4 Catalog of High Energy X-Ray Sources", ApJSupp, 54, 581-617 (1984).

2. Wood, K.S. et al., "The HEAO A-1 X-Ray Source Catalog", ApJSupp, 56, 507 (1984).

3. Piccinotti, G. et al., "A Complete X-Ray Sample of the High Latitude($|b|>20°$) Sky From HEAO 1 A-2: Log N-Log S and Luminosity Functions", ApJ, 253, 485-503 (1982).

4. Harmon, B.A. et al., "BATSE Observations of Transient Hard X-Ray Sources", The Second Compton Symposium, AIP Conference Proceedings, eds C.E. Fichtel, N. Gehrels, and J.P. Norris, (AIP Press: New York), 304, 210-219 (1994).

5. Trümper, J., "First Results From the ROSAT All-Sky Survey", Frontiers in X-ray Astronomy, eds Tanaka, Y. and Koyama, K., (Universal Academy Press, Inc.: Tokyo), 185-192 (1992).

6. Antonucci, R. "Unified Models For Active Galactic Nuclei And Quasars", Annu. Rev. Astron. Astrophys, 31, 473-521 (1993).

7. Nagase, F., "Accretion Powered X-Ray Pulsars", PASJ, 41, 1-79 (1989).

8. Nagase, F., "X-Ray Properties of X-Ray Pulsars", Frontiers of X-ray Astronomy, eds Tanaka, Y. and Koyama, K., (Universal Academy Press, Inc. Tokyo), 79-90 (1992).

9. Priedhorsky, W.C. and Holt, S.S., "Long-Term Cycles in Cosmic X-Ray Sources", Space Sci Rev, 45, 291-348 (1987).

10. Fishman, G.J., "Gamma-Ray Bursts: Ovservational Overview", The Second Compton Symposium, AIP Conference Proceedings, eds C.E. Fichtel, N. Gehrels, and J.P. Norris, (AIP Press: New York), 304, 22-29 (1994).

11. Butler, J.F. et.al., "Progress in CdZnTe Radiation Detectors", Proc. Mat. Res. Soc. Annual Meeting, April 12-16, San Francisco (1993).

12. Doty, F.P. et al., "X-Ray and Gamma-Ray Imaging in Monolithic CdZnTe Detector Arrays", SPIE Vol. 1945, 145-151 (1993).